

## SCREENING AND VERIFICATION OF DIFFERENTIAL DNA METHYLATION GENES IN THE PERIPHERAL BLOOD CELLS OF CHILDREN WITH SKELETAL FLUOROSIS IN GUIZHOU PROVINCE OF CHINA

Jie Deng,<sup>a,b,c</sup> Xiao-Xiao Zeng,<sup>b,c</sup> Xian-Hong Liu,<sup>b,c</sup> Dan Chen,<sup>a,b</sup> Yang-Ting Dong,<sup>b,c</sup> Hui Song,<sup>b,c</sup> Yi Li,<sup>b,c</sup> Zhi-Zhong Guan<sup>a,b,c,\*</sup>

Guiyang, Guizhou Province, People's Republic of China

**ABSTRACT:** The levels of DNA methylation were analyzed in the peripheral blood cells of children, with or without skeletal fluorosis, in the area of the coal-burning type of endemic fluorosis in Guizhou Province of China. Whole genome DNA methylation 450 K BeadChip and pyrosequencing were performed, and the main function and pathway of differential methylation genes determined by GO analysis and the KEGG database. The results showed that 15 differential hypermethylated and 22 hypomethylated CpG sites were determined in the children with skeletal fluorosis, which involved 29 known genes, as compared to controls. The majority of the differentially methylated CpG loci resided in the gene body. Further, the GO analysis and the KEGG database for the pathway analysis indicated that these differential genes are mainly involved in synapse maturation, axon, neuron projection membrane, transcription coactivator activity, and the Notch signaling pathway. Pyrosequencing analysis showed that the gene MAML2 was hypomethylated in the children with skeletal fluorosis, which is the same as the chip result. A change concerning genome-wide DNA methylation in the children with skeletal fluorosis was also found. The results suggest that the alteration of the hypomethylated MAML2 gene may play an important role in the occurrence and development of skeletal fluorosis.

Key words: Children; DNA Methylation; Endemic fluorosis; Pyrosequencing; Skeletal fluorosis

### INTRODUCTION

Endemic fluorosis occurs as a result of excess fluoride intake due to environmental factors and induces damages to the human body characterized by a vast array of symptoms and pathological changes in addition to the typical skeletal or dental fluorosis.<sup>1-2</sup> In Guizhou Province of China, fluorosis occurs due to the contamination of food and air by burning coal containing a high level of fluoride in non-flued stoves<sup>3</sup>.

DNA methylation, an epigenetic modification, is a process in which a methyl group is added to a region where a cytosine nucleotide is located next to a guanine nucleotide that is linked by a phosphate.<sup>4</sup> CpG islands (CpGIs) are methylated by a group of enzymes called DNA methyltransferases. Classically, insertion of methyl groups at CpGIs is thought to block the binding of transcription factors to promoters and therefore results in repressed gene expression. More recent investigations have demonstrated that DNA methylation in other regions of the genome, including the gene bodies, are likely to influence gene expression, thus necessitating a comprehensive analysis of all DNA methylation sites.<sup>5-6</sup> DNA methylation has been used to reflect environmentally induced epigenomic reprogramming and to analyze

<sup>a</sup>Department of Pathology at the Affiliated Hospital of Guizhou Medical University; <sup>b</sup>Key Laboratory of Endemic and Ethnic Diseases of the Ministry of Education (Guizhou Medical University); <sup>c</sup>Key Laboratory of Medical Molecular Biology, Guiyang, People's Republic of China; \*For correspondence: Zhi-Zhong Guan, Department of Pathology at the Affiliated Hospital of Guizhou Medical University, Guiyang 550004, Guizhou, People's Republic of China; E-mail: 1457658298@qq.com or zhizhongguan@yahoo.com

the risk of diseases.<sup>7</sup> Aberrant DNA methylation, which may lead to genomic instability and altered gene expression, is frequently observed.<sup>8</sup> DNA methylation transferase 1 (DNMT1) is considered to be responsible for the maintenance of genomic methylation patterns. In the peripheral blood of patients with endemic fluorosis induced by coal burning, the elevated DNMT1 expression of its transcription and protein is involved in the expression of the human osteoblast related gene and could be the early molecular events of skeletal fluorosis.<sup>9</sup> Recently, a changed methylation of the MGMT and MLH1 genes in the blood of the patients living in such fluorosis area and the blood and liver of rats with chronic fluorosis has been observed, which indicates that the modified methylation of MGMT and MLH1 genes caused by fluoride may result in liver damage.<sup>10</sup>

In recent years, a survey in the area of endemic fluorosis in Guizhou carried out by our group indicated that many patients with skeletal fluorosis occurred at a younger age (data not shown). Among them, some cases developed spinal rigidity, joint fractures, and even disability in adulthood, although the clinical manifestations in childhood did not show any obvious evidence that the further development of severe skeletal fluorosis was likely.<sup>11</sup> Therefore, it may be interesting to explore the possibility that there may be a biomarker that gives an early warning of the later development of severe skeletal fluorosis and, if present, to reveal the mechanism. This aim of the present study was to analyze DNA methylation from the whole genome level in peripheral white blood cells from the children living in the area of the coal burning type of skeletal fluorosis by using the high resolution Infinium 450 K methylation array.

## MATERIALS AND METHODS

*Investigated subjects:* Sixteen patients (4 females and 12 males), the average age of whom was  $11.50 \pm 0.88$  years old, with chronic fluorosis were selected in Shuicheng county of Guizhou Province (the area of coal-burning type of endemic fluorosis). These patients with skeletal fluorosis were determined by imageological examination. All of the children had dental fluorosis and their mean urinary fluoride content was  $1.02 \pm 0.45$  ppm. At the same time, 16 children (9 females and 7 males), without dental or skeletal fluorosis and with no other obvious chronic diseases, were selected from the same area. Their average age was  $11.75 \pm 1.06$  years old and their mean urinary fluoride content was  $0.56 \pm 0.16$  ppm. Blood samples were obtained from all the participants who had given written informed consent. The study design was approved by the ethics committee of the Guizhou Medical University of China. All of the children provided about 2 mL of fasting venous blood for examination.

*Analysis of the fluoride concentrations in the urine using the fluoride ion selective electrode:* Biomarkers of  $F^-$  exposure can be evaluated using several biological tissues or fluids (i.e., teeth, bone, nail, hair, plasma, urine, and saliva).<sup>12</sup> Urine is the main pathway of  $F^-$  elimination from the body, and excretion by the urinary system is proportional to the total  $F^-$  intake.<sup>13</sup> The analysis of fluoride concentrations in the urine is one of the most commonly used methods for determining the level of accumulation of fluorine in the body and the severity of fluorosis.

Early morning spot urine samples of every child were collected in polyethylene containers and stored at  $-20^\circ\text{C}$  until analysis. The detection limit of the  $F^-$  selective electrode (PF-202-CF, INESA, Shanghai) was 0.01 ppm. During the measurement,

TISAB II was used to adjust the pH and ionic strength of the standards and the urine samples. Double-distilled deionized water was used throughout the experiment. The concentration was quantified against a fluoride calibration curve in a range of 0.1 to 20 ppm prepared with a reagent blank. The measurement accuracy of the ion selective electrode ranged from 97.3% to 101.9% relative to the standard fluoride solution, with the measurement errors less than  $\pm 5\%$ , and the recovery rate from 93.4% to 108.3%.<sup>14</sup>

*Infinium DNA methylation analysis:* Genome-wide methylation analysis was performed with the Infinium HD Methylation 450K BeadChip (Illumina Inc., USA) interrogating about 480,000 CpGs distributed in promoters, gene bodies, 3'UTRs, and intergenic regions.<sup>15</sup> Bisulfite conversion of DNA was carried out using the EZ DNA Methylation Kit (Zymo Research, Orange, CA, USA) following the manufacturer's procedure, but with the modifications described in the Infinium Assay Methylation Protocol Guide. Processed DNA samples were then hybridized to the BeadChip following the Illumina Infinium HD Methylation Protocol.<sup>16</sup>

DNA methylation data were processed using GenomeStudio software. Individual probe  $\beta$  values (range 0–1) are approximate representations of the absolute methylation percentage of specific CpG sites within the sample population. Beta ( $\beta$ )=1 indicates complete methylation;  $\beta$ =0 represents no methylation. The values were derived by comparing the ratio of intensities between the methylated and unmethylated alleles using the following formula:

$$\beta \text{ value} = \frac{\text{Max (Signal B, 0)}}{\text{Max (Signal A, 0) + Max (Signal B, 0) + 100}}$$

Where Signal B is the array intensity value for the methylated allele and Signal A is the array intensity value for the nonmethylated allele.

The samples were processed using the Bioconductor package, which is specifically designed for Illumina data.<sup>17</sup>

*Hierarchical clustering:* To ascertain whether these differentially hypomethylated and hypermethylated genes among the groups were selected correctly, hierarchical cluster analysis was performed based on differentially expressed genes using Cluster Treeview software from Stanford University.

*Gene ontology analysis and pathway analysis:* Gene ontology analysis was applied to analyze the main function of differential methylation genes according to the Gene ontology project.<sup>18</sup> Fisher's exact test and  $\chi^2$  tests were used to classify the GO category, and the FDR was calculated to correct the  $P$  value.<sup>19</sup> The standard of difference screening was  $P < 0.05$ . Similarly, pathway analysis was used to find out the significant pathway of the differential genes according to KEGG. Fisher's exact test and  $\chi^2$  tests were used to select the significant pathway, and the threshold of significance was defined by the  $P$  value and FDR<sup>20</sup>. The standard of difference screening was  $P < 0.05$ .

*Pyrosequencing:* Pyrosequencing assays were performed for all of the study samples on a PyroMarkQ96 ID using PyroMark Gold reagents (Qiagen, Valencia, CA, USA).<sup>21</sup> Primers for ATF6, MAML2, BMP8B, MAML3, targeting 8 CpGs in the gene body, promoter, 3'UTR, and the gene body, respectively, were generated

according to the PyroMark Assay Design software version 2.0 (Qiagen, Valencia, CA, USA). The primer sequences are listed in Table 1.

**Table 1.** Pyrosequencing primer sequences

Gene	Primer	Primer sequence (5' to 3')	CpG Sites
ATF6	Sense	TTGGAAAGATGAAAAGAGGTAGATAAAG	1
	Antisense	Biotin-ATACCTCTACAAAACCACTCACTA	
	Sequencing	GAAAAGAGGTAGATAAAGAAG	
MAML2	Sense	GTGGTATTAGTTTTTATTAGGGAGTTT	5
	Antisense	Biotin-CCATCCCCCACCATAAATCTAAAAATCT	
	Sequencing	GAGTATAATGAAAGTTTGTGTA	
BMP8B	Sense	TTTTTTGGTTAGGTGTATTTGATGA	1
	Antisense	Biotin-AATCCTCCCTAACAATACCC	
	Sequencing	ACTAAATTTAAAAATTCCTACTTC	
MAML3	Sense	TAGGGGTGTGATTGTGGTTAT	1
	Antisense	Biotin-ACAAAATAAACTCCCACCTTTAATAAT	
	Sequencing	ATTGGAGTTTAGGTTTTTTAGA	

PCR reactions were performed in a total volume of 50  $\mu$ L containing 5X buffer GC, 10 mM dNTPs, 50 pM of each primer, 1.0 U Taq polymerase and 2  $\mu$ L of bisulfite modified DNA with the following profile: 95°C for 3 min followed by 40 cycles of denaturation at 94°C for 30 sec, annealing at 54°C for 30 sec, and extension at 72°C for 1 min. Extension at 72°C for 7 min was finally performed. According to the Pyrosequencing software sequence design information, the substrate mixture, the enzyme mixture and dNTPs (Qiagen, Valencia, CA, USA) were sequentially added to the reagent compartment. The reagent chamber and the 96-well reaction plate were placed in a PyroMark Q96 ID for reaction, and the Pyro Q-CpG software automatically analyzed the methylation status of each site.<sup>22</sup>

The pyrosequencing data were analyzed with the Mann-Whitney U test to identify statistical differences between the cases and the healthy controls.

Infinium DNA methylation analysis was performed on the blood of three controls and three cases while pyrosequencing was carried out on the samples from 16 controls and 16 cases (Table 2).

## RESULTS

*The differentially hypomethylated or hypermethylated CpG patterns associated with skeletal fluorosis and functional analysis:* Differences in the DNA methylation levels at 37 sites between the children with skeletal fluorosis and the controls were observed in the study. Hierarchical cluster analysis showed 22 differentially hypomethylated and 15 hypermethylated CpG sites in the children with skeletal fluorosis (Figure 1A), which involved 29 known genes (Tables 3 and 4).

**Table 2.** Summary of experimental groups used in the examination of microarray-based DNA methylation and pyrosequencing (I°=dental fluorosis present in the primary dentition; II°=dental fluorosis present in the permanent dentition)

Experiment	Group	n	Age (Years±SD)	Urinary fluoride (mg/L)	Skeletal fluorosis (n)		
					Normal	I°	II°
DNA methylation (450k BeadChip)	Control	3	10.67±0.89	0.65±0.22	3	0	0
	Case	3	12.00±0.00	0.94±0.22	0	3	0
Pyrosequencing	Control	16	11.75±1.06	0.56±0.16	16	0	0
	Case	16	11.50±0.88	1.02±0.45	0	15	1

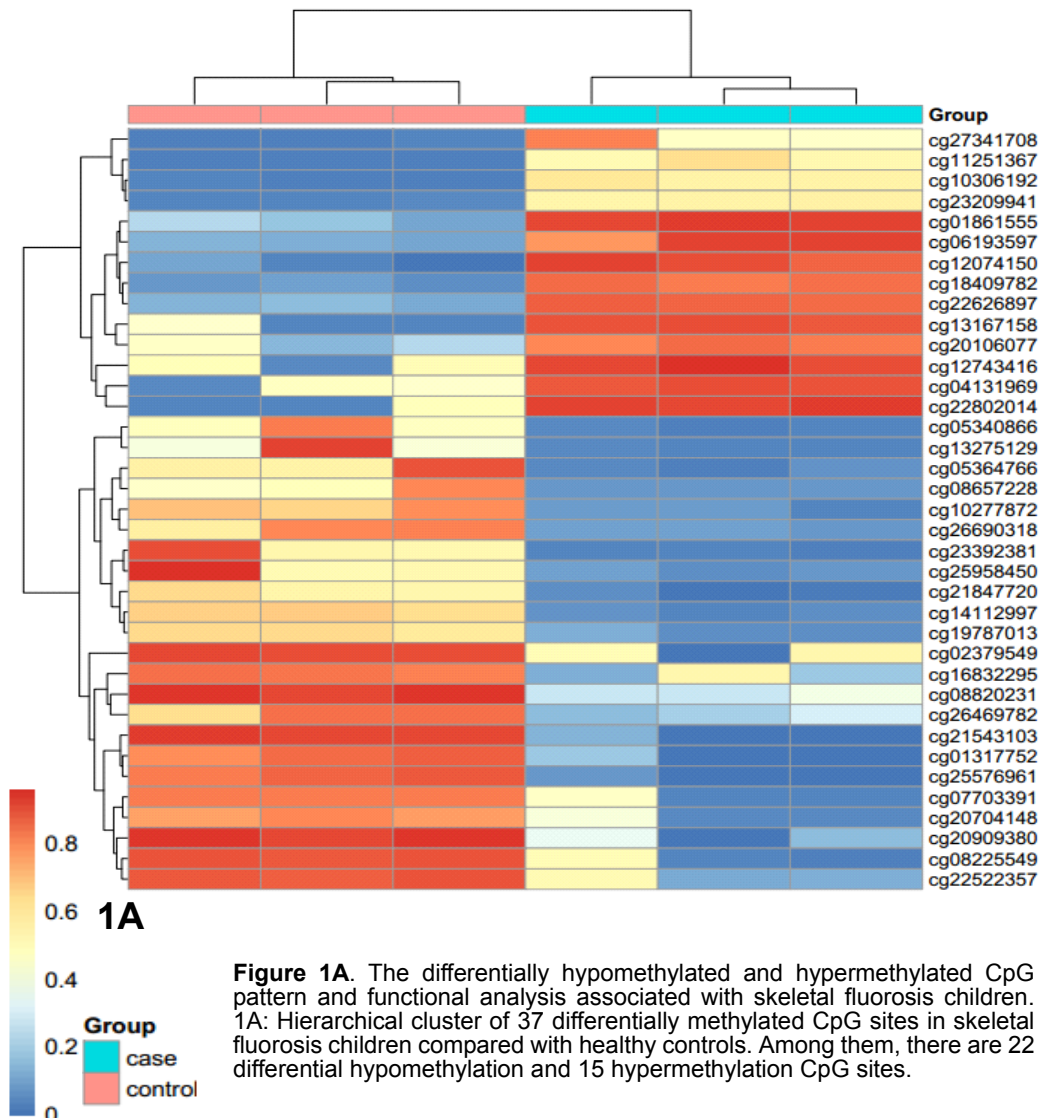


**Figure 1A.** The differentially hypomethylated and hypermethylated CpG pattern and functional analysis associated with skeletal fluorosis children. 1A: Hierarchical cluster of 37 differentially methylated CpG sites in skeletal fluorosis children compared with healthy controls. Among them, there are 22 differential hypomethylation and 15 hypermethylation CpG sites.

**Table 3.** The differentially hypomethylated genes involved in skeletal fluorosis children

Gene symbol	Gene symbol description	Chromo -some	Average Beta	P Value
POLS	Polymerase (DNA directed) sigma	5	0.87950	4.60E-08
TTC23	Tetratricopeptide repeat domain 23	15	0.83620	3.43E-07
IL17RA	Interleukin 17 receptor A	22	0.62255	2.85E-06
SLC26A10	Solute carrier family 26, member 10	12	0.63060	4.87E-06
VCX	Variable charge, X-linked	X	0.78489	8.27E-06
RECQL4	RecQ protein-like 4	8	0.56332	3.24E-05
PYROXD2	Pyridine nucleotide-disulphide oxidoreductase domain 2	10	0.65411	4.22E-05
CNTNAP2	Contactin associated protein-like 2	7	0.56788	0.0002085
CTNNA2	Catenin (cadherin-associated protein), alpha 2	2	0.63198	0.000343
MYOM2	Myomesin (M-protein) 2	8	0.56544	0.000567
ATF6	Activating transcription factor 6	1	0.62925	0.0016141
PALM	Paralemmin	19	0.54837	0.0032168
MAML2	Mastemind-like 2	11	0.54787	0.0034674
C6orf89	Chromosome 6 open reading frame 89	6	0.55471	0.0041849
ZNF681	Zinc finger protein 681	19	0.60106	0.0043057
SLCO2B1	Solute carrier organic anion transporter family, member 2B1	11	0.61133	0.004318
STMN2	Stathmin-like 2	8	0.70370	0.0051124
BMP8B	Bone morphogenetic protein 8b (osteogenic protein 2)	1	0.64932	0.0062858

The differential sites of DNA methylation are evenly distributed on chromosomes. DNA methylation differences occurred not only in the CpG islands of the promoter region, but also in areas such as the CpG islands and the CGI shelves located at a certain distance from the gene flanking sequence. GO analysis indicates that these differential methylation genes are mainly involved in synapse maturation, axon, neuron projection membrane, transcription coactivator activity, and the Notch signaling pathway (Figure 1B).

**Table 4.** The differentially hypermethylated genes involved in skeletal fluorosis children

Gene symbol	Gene symbol description	Chromosome	Average Beta	P Value
DISC1	Disrupted in schizophrenia 1	1	-0.53383	8.56E-09
SMYD3	SET and MYND domain containing 3	1	-0.73753	3.57E-08
MMP27	Matrix metalloproteinase 27	11	-0.55868	7.54E-08
FMN2	Formin 2	1	-0.54666	2.18E-07
MAML3	Mastermind-like 3	4	-0.56110	1.45E-04
DEFB128	Defensin, beta 128	20	0.52599	0.0004491
WDR27	WD repeat domain 27	6	-0.54991	9.56E-04
MIB2	Mindbomb homolog 2	1	-0.72224	0.0026317
SNRNP40	Small nuclear ribonucleoprotein 40kDa (U5)	1	-0.73462	0.0028697
TRIM24	Tripartite motif-containing 24	7	-0.57140	0.0084788
MYADML	Myeloid-associated differentiation marker-like	2	-0.56994	0.0088229

*Genomic distribution of the differentially methylated CpG sites associated with skeletal fluorosis with respect to functional genomic distribution and CpG content:* The location of the differentially methylated CpG loci associated to the children with skeletal fluorosis with respect to the functional genomic distribution (promoter, gene body, 3'UTR, and intergenic) and the CpG content (CpG island, shore, shelf, and open sea) was similar in the study here, and the majority of the CpG loci were residing in the gene bodies (Figure 2A) and in the open seas (Figure 2B).

*Pathway analysis of the differentially methylated genes associated with skeletal fluorosis:* For further investigating the key pathways linked to these distinct genes, an analysis was performed of the significant pathway categories ( $P < 0.05$ ) of the significant differential genes associated with skeletal fluorosis. Our analysis showed that these differentially methylated genes were distributed in 4 significant pathways, including the Notch signaling pathway, the Spliceosome, the Hippo signaling pathway, and the Dorso-ventral axis formation (Figure 3 and Table 5).

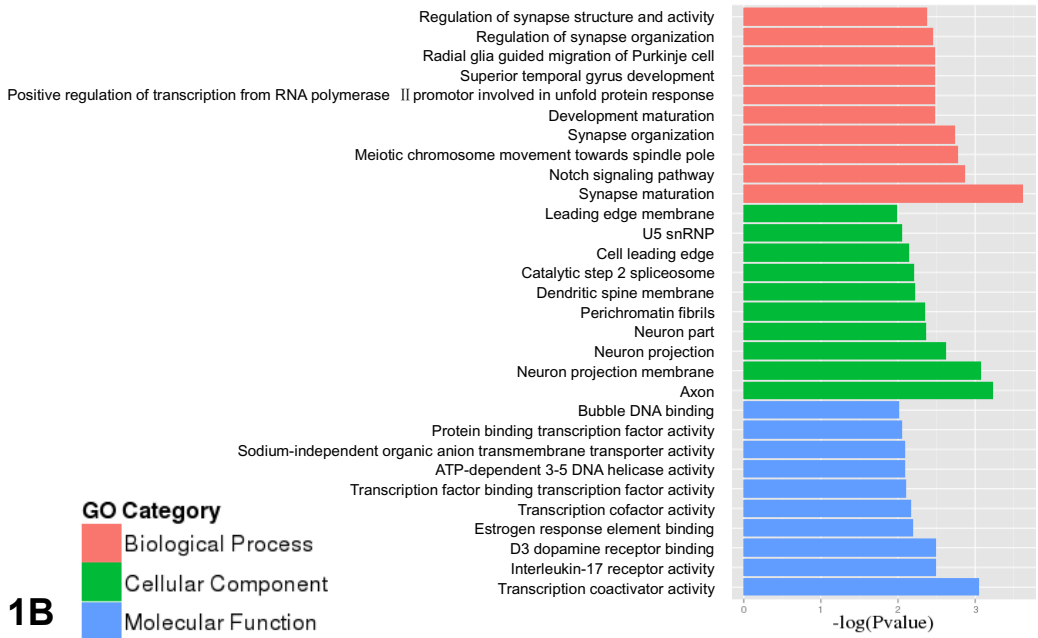
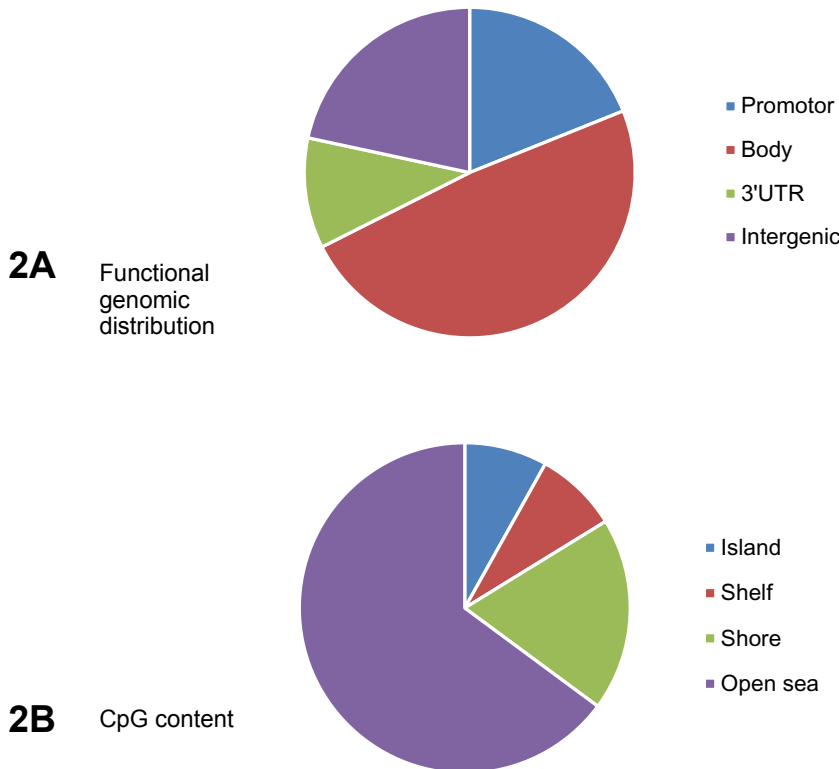


**Figure 1B.** The differentially hypomethylated and hypermethylated CpG pattern and functional analysis associated with skeletal fluorosis in children. 1B: GO analysis of the differential methylation genes in children with skeletal fluorosis compared to healthy controls.



**Figures 2A and 2B.** Genomic distribution of the differentially methylated CpGs sites in the children with skeletal fluorosis as compared to the healthy controls. 2A: Functional genomics distribution (promoter, gene body, 3'UTR, and intergenic); 2B: CpG content (CpG island, shore, shelf, and open sea).

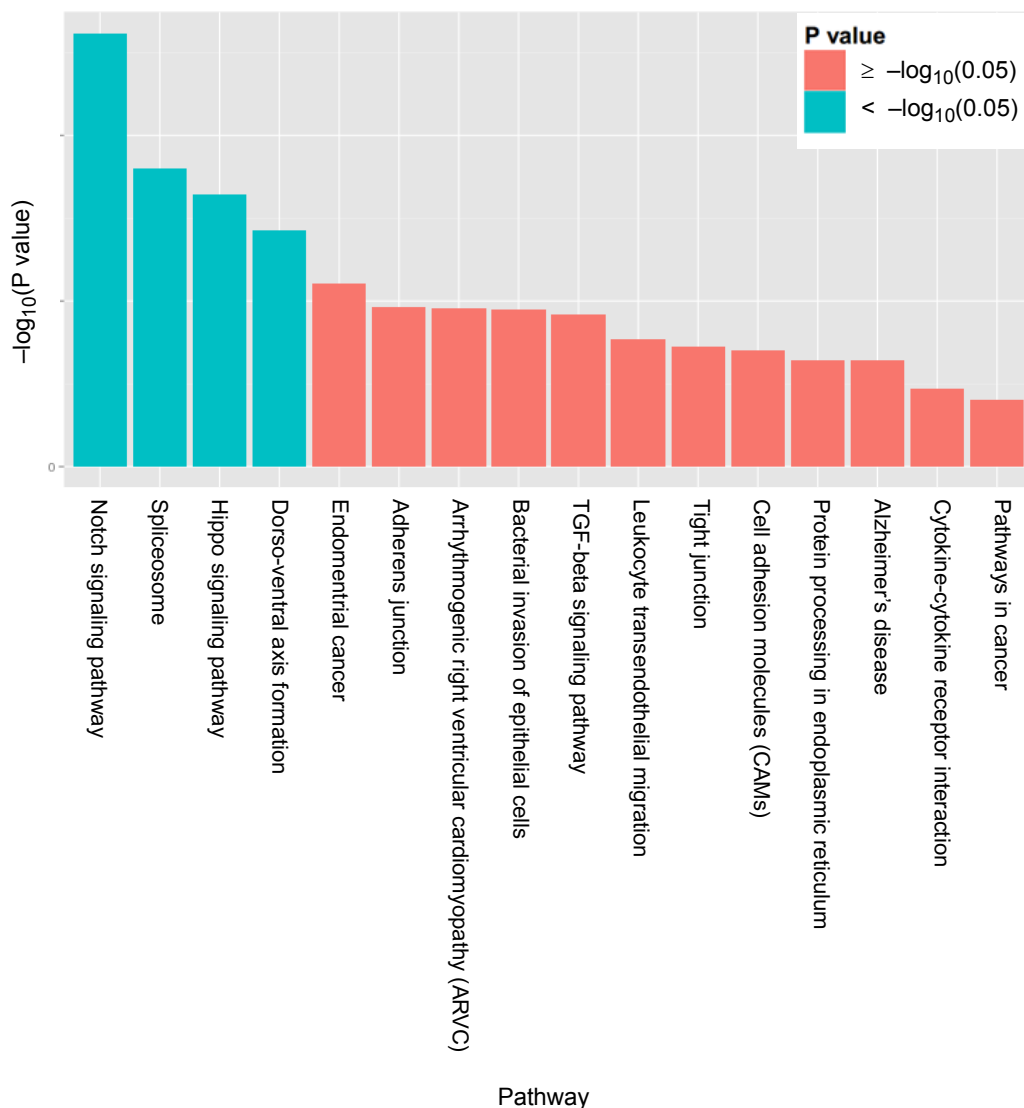


**Figure 3.** Histogram of the signal pathways of the differential methylation genes in children with skeletal fluorosis. X axis: the name of the pathway; Y axis: negative logarithm of the P value ( $-\log_{10} P$ ). The larger the value, the smaller the P value.

*Verification of 450 K methylation data by pyrosequencing:* To confirm the 450 K BeadChip data, 8 CpG sites located in 4 genes that might be relevant to bone metabolism related diseases were selected for a confirmation by pyrosequencing. The differences in the DNA methylation levels between the skeletal fluorosis cases and the controls for these selected CpG sites exhibited a similar magnitude to that observed with the 450 K BeadChips, in which, however, only 3 CpG sites on MAML2 were shown to have statistical significance (Table 6)

**Table 5.** Path-net analysis of differentially methylated genes associated with skeletal fluorosis in children

Pathway	Gene symbol	Methylation style	P value
Notch signaling pathway	MAML2 and MAML3	Low/High	0.002
Spliceosome	SNRNP40	High	0.016
Hippo signaling pathway	BMP8B and CTNNA2	Low	0.023
Dorso-ventral axis formation	FMN2	High	0.037

**Table 6.** The detection rate of methylation in CpG islands of the differential methylation genes

Gene symbol	CpG island	The rate of methylation		P values
		Control (n=16)	Cases (n=16)	
ATF6	CpG1	66.66±29.45	60.29±37.39	P>0.05
	CpG1	3.53±3.95	0.37±1.49	p<0.05
	CpG2	5.23±4.17	1.86±3.44	p<0.05
MAML2	CpG3	10.95±3.59	3.44±2.41	P>0.05
	CpG4	6.18±3.42	1.40±3.03	P<0.01
	CpG5	2.15±4.80	1.21±3.32	P>0.05
BMP8B	CpG1	52.82±25.81	54.00±24.22	P>0.05
MAML3	CpG1	21.24±19.37	23.33±25.06	P>0.05

The values are shown as the mean±SD of each independent experiment. The P values are as compared to the controls.

## DISCUSSION

Endemic skeletal fluorosis, a chronic metabolic disease of bones and joints, is a health problem worldwide. In recent years, areas with the coal-burning type of endemic fluorosis have adopted many methods to prevent and cure fluorosis. However, an efficient treatment of skeletal fluorosis has not been obtained. Therefore, it is of critical important to understand better the condition of skeletal fluorosis and the mechanisms involved in its pathogenesis. It is now known that epigenetic modifications, including DNA methylation, histone modification, and noncoding RNA, can occur in response to chemical exposure and may be involved in the pathogenic effects of environmental chemicals, by regulating the expression of specific genes.<sup>23-25</sup> Among them, DNA methylation alterations have been found repeatedly following exposure to various environmental chemicals, including benzene,<sup>17</sup> phenol and hydroquinone,<sup>26</sup> and dioxidine,<sup>27</sup> suggesting that DNA methylation is inducible by chemical exposures. DNA methylation changes may be early biomarkers for chemical induced toxic effects.

In our study, DNA methylation profiles from the peripheral blood cells of children with skeletal fluorosis were compared to control children to try to gain new biomarkers for the skeletal fluorosis affected children living in an area of the burning type of endemic fluorosis. By integrating the DNA methylation and pyrosequencing data of differentially methylated genes, we found that the hypomethylated MAML2 gene might be a potential biomarker for skeletal fluorosis in the children in this area.

In previous studies, DNA methylation alterations in p16 and c-Fos were observed in cultured cells treated by fluoride.<sup>28-29</sup> Fluorosis increased DNA methylation of the NNAT gene and decreased its expression, which disturbs the glucose transport in porcine oocytes.<sup>30</sup> In addition, fluoride disrupted DNA methylation of H19 and Peg3 imprinted genes during the early development of mouse embryo.<sup>31-32</sup> These results suggest that chronic fluoride poisoning may be mediated in part by DNA methylation, which can substantially affect gene transcription without changing the DNA sequence.

The methylation of genes from peripheral blood cells is commonly associated with many kinds of diseases.<sup>27,33</sup> Our latest study indicated a change of the DNA repair gene MGMT and MLH1 methylation in the blood of the adult patients and rats with chronic fluorosis, which may play a role in the damage of liver caused by fluoride.<sup>10</sup> In this study, we performed genome-wide DNA methylation analyses on blood DNA samples from the children with skeletal fluorosis and controls, which indicated that the differences of DNA methylation occur not only in the CpG islands of the promoter region, but also in the areas, such as the CpG islands and CGI shelves, located at a certain distance from the gene flanking sequence. While the role of DNA methylation in the promoter and CpG island regions has been appreciated, the importance of DNA methylation in the gene body and the shore regions for transcription regulation has only recently come to attention.<sup>34-35</sup>

In addition, we collected 8 CpG sites located in 4 genes that might be relevant to bone metabolism, which were confirmed by pyrosequencing. MAML2 and MAML3 are the numbers of the mastermind-like gene family and they function efficiently as transcriptional coactivators for Notch receptors.<sup>36</sup> The study of both of these genes has mainly focused on cell development and some cancers.<sup>37-38</sup> However, the

importance of Notch signaling in skeletogenesis and bone homeostasis has long been suggested through a number of studies.<sup>39-40</sup> Moreover, the BMP superfamily signaling has become one of the most heavily investigated topics in vertebrate skeletal biology. Whereas a large part of this research has focused on the roles of BMP2, BMP4, and BMP7 in the formation and repair of endochondrial bone, a large number of BMP superfamily molecules have now been implicated in almost all aspects of bone, cartilage, and joint biology.<sup>41</sup> ATF6 is an endoplasmic reticulum (ER) stress-regulated transmembrane transcription factor that activates the transcription of ER molecular chaperones. Upon ER stress, membrane-bound ATF6 is cleaved and translocated from the ER to the nucleus, where it up-regulates unfolded protein response (UPR)-related genes.<sup>42</sup> The UPR is possibly involved in the mechanism of the osteoblast differentiation induced by fluoride.<sup>43</sup> Thus, we assumed that the differential methylation of the coactivator MAML2/3, BMP8B, and ATF6 may play a role in skeletal fluorosis. By pyrosequencing differences in the level of DNA methylation between the skeletal fluorosis cases and the controls, we found that these selected CpG sites exhibited a similar magnitude as observed with the 450 K BeadChips, even though the differences were statistically significant for only 3 CpG sites on MAML2.

### CONCLUSION

In conclusion, a change involving genome-wide DNA methylation in the children with skeletal fluorosis was found, which suggests that the alteration of hypomethylated MAML2 may play an important role in the occurrence and development of skeletal fluorosis.

### ACKNOWLEDGMENTS

This work was financed by grants from the National Natural Science Foundation of China (U1812403) and the Scientific Foundations of Guizhou Province of China (TJ18037, [2018]187, 2014-06, 2014-6008, 2016-4001).

### REFERENCES

- 1 Guan ZZ. Coal-burning type of endemic fluorosis. Beijing: People's Medical Publishing House of China; 2015. pp. 1-2.
- 2 Viswanathan G, Jaswanth A, Gopalakrishnan S, Sivailango S. Mapping of fluoride endemic areas and assessment of fluoride exposure. *Sci Total Environ* 2009;407:1579-87.
- 3 Zhang T, Shan KR, Tu X, He Y, Pei JJ, Guan ZZ. Myeloperoxidase activity and its corresponding mRNA expression as well as gene polymorphism in the population living in the coal-burning endemic fluorosis area in Guizhou of China. *Biol Trace Elem Res*. 2013;152:379-6.
- 4 Jones PA. Functions of DNA methylation: Islands, start sites, gene bodies and beyond. *Nat Rev Genet* 2012;13(7):484-92.
- 5 Zaina S, Heyn H, Carmona FJ, Varol N, Sayols S, Condom E, et al. DNA methylation map of human atherosclerosis. *Circ Cardiovasc Genet* 2014;7(5):692-700.
- 6 Yang X, Han H, De Carvalho DD, Lay FD, Jones PA, Liang G. Gene body methylation can alter gene expression and is a therapeutic target in cancer. *Cancer Cell* 2014;26(4):577-90.
- 7 Hou L, Zhang X, Tarantini L, Nordio F, Bonzini M, Angelici L, et al. Ambient PM exposure and DNA methylation in tumor suppressor genes: a cross-sectional study. *Part Fibre Toxicol* 2011;8:25.

- 147 Research report  
Fluoride 52(2):135-148.  
April 2019
- DNA methylation in children with skeletal fluorosis  
Deng, Zeng, Liu, Chen, Dong, Song, Li, Guan 147
- 8 Kuang SQ, Tong WG, Yang H, Lin W, Lee MK, Fang ZH, et al. Genome-wide identification of aberrantly methylated promoter associated CpG islands in acute lymphocytic leukemia. *Leukemia* 2008;22(8):1529-38.
  - 9 Liao YD, Zhou J, Qiu B, Liao YF, Yan WM, Zhang AH, et al. DNA Methylation Transferase 1 transcription and protein expression in peripheral blood of patients with endemic Fluorosis Induced by Coal Burning. *J Environ Occup Med.* 2014;32(12):941-3.
  - 10 Wu CX, Wang YH, Li Y, Guan ZZ, Qi XL. Changes of DNA repair gene methylation in blood of chronic fluorosis patients and rats. *J Trace Elem Med Biol* 2018;50:223-8.
  - 11 Wang XH, Yu MJ. Case-control study of risk factors for fired skeletal fluorosis in children. *Mod Prevent Med* 2016;42(13):2184-6, 2193.
  - 12 Whitford GM. Monitoring fluoride exposure with fingernail clippings. *Schweiz Monatsschr Zahnmed* 2005;115(8):685-9.
  - 13 Whitford GM. The metabolism and toxicity of fluoride. *Monogr Oral Sci* 1996;16:1-153.
  - 14 Yu X, Chen J, Li Y, Liu H, Hou C, Zeng Q, et al. Threshold effects of moderately excessive fluoride exposure on children's health: A potential association between dental fluorosis and loss of excellent intelligence. *Environ Int* 2018;118:116-24.
  - 15 Bibikova M, Barnes B, Tsan C, Ho V, Klotzle B, Le JM, et al. High density DNA methylation array with single CpG site resolution. *Genomics* 2011;98(4):288-95.
  - 16 Urdinguio RG, Bayón GF, Dmitrijeva M, Toraño EG, Bravo C, Fraga MF, et al. Aberrant DNA methylation patterns of spermatozoa in men with unexplained infertility. *Hum Reprod* 2015;30(5):1014-28.
  - 17 Yang J, Bai W, Niu P, Tian L, Gao A. Aberrant hypomethylated STAT3 was identified as a biomarker of chronic benzene poisoning through integrating DNA methylation and mRNA expression data. *Exp Mol Pathol* 2014;96(3):346-53.
  - 18 Ashburner M, Ball CA, Blake JA, Botstein D, Butler H, Cherry JM, et al. Gene ontology: tool for the unification of biology. *Nat Genet* 2000;25(1):25-9.
  - 19 Dupuy D, Bertin N, Hidalgo CA, Venkatesan K, Tu D, Lee D, et al. Genome-scale analysis of *in vivo* spatiotemporal promoter activity in *Caenorhabditis elegans*. *Nat Biotechnol* 2007;25(6):663-8.
  - 20 Draghici S, Khatri P, Tarca AL, Amin K, Done A, Voichita C, et al. A systems biology approach for pathway level analysis. *Genome Res* 2007;17(10):1537-45.
  - 21 Barchitta M, Quattrocchi A, Maugeri A, Canto C, La Rosa N, Cantarella MA, et al. LINE-1 hypermethylation in white blood cell DNA is associated with high-grade cervical intraepithelial neoplasia. *BMC Cancer* 2017;17(1):601.
  - 22 Delaney C, Garg SK, Yung R. Analysis of DNA Methylation by Pyrosequencing. *Methods Mol Biol* 2015;1343:249-64.
  - 23 Daiwile AP, Sivanesan S, Tarale P, Naoghare PK, Bafana A, Parmar D, et al. Role of fluoride induced histone trimethylation in development of skeletal fluorosis. *Environ Toxicol Pharmacol* 2018;57:159-65.
  - 24 Suzuki M, Ikeda A, Bartlett JD. Sirt1 overexpression suppresses fluoride-induced p53 acetylation to alleviate fluoride toxicity in ameloblasts responsible for enamel formation. *Arch Toxicol* 2018;92(3):1283-93.
  - 25 Zhang A, Li H, Xiao Y, Chen L, Zhu X, Li J, et al. Aberrant methylation of nucleotide excision repair genes is associated with chronic arsenic poisoning. *Biomarkers* 2017;22(5):429-38.
  - 26 Li Y, Wu XR, Li XF, Suriguga, Yu CH, Li YR, et al. Changes in DNA methylation of erythroid-specific genes in K562 cells exposed to phenol and hydroquinone. *Toxicology* 2013;312:108-14.

- 148 Research report  
Fluoride 52(2):135-148.  
April 2019
- DNA methylation in children with skeletal fluorosis  
Deng, Zeng, Liu, Chen, Dong, Song, Li, Guan 148
- 27 Smirnikhina SA, Voronina ES, Lavrov AV, Bochkov NP. Dioxidine-induced changes in genome-wide DNA methylation in a culture of peripheral blood lymphocytes. *Bull Exp Biol Med* 2013;155(2):224-7.
- 28 Wu S, Yan W, Qiu B, Liao Y, Gu J, Wei S, et al. Aberrant methylation-induced dysfunction of p16 is associated with osteoblast activation caused by fluoride. *Environ Toxicol* 2018;1-11.
- 29 Niu Q, Liu H, Guan Z, Zeng Q, Guo S, He P, et al. The effect of c-Fos demethylation on sodium fluoride-induced apoptosis in L-02 cells. *Biol Trace Elem Res* 2012;149(1):102-109.
- 30 Liu X, Nie ZW, Gao YY, Chen L, Yin SY, Zhang X, et al. Sodium fluoride disturbs DNA methylation of NNAT and declines oocyte quality by impairing glucose transport in porcine oocytes. *Environ Mol Mutagen* 2018;59(3):223-33.
- 31 Zhu JQ, Si YJ, Cheng LY, Xu BZ, Wang QW, Zhang X, et al. Sodium fluoride disrupts DNA methylation of H19 and Peg3 imprinted genes during the early development of mouse embryo. *Arch Toxicol* 2014;88(2):241-8.
- 32 Zhao L, Zhang S, An X, Tan W, Tang B, Zhang X, et al. Sodium Fluoride Affects DNA methylation of imprinted genes in mouse early embryos. *Cytogenet Genome Res* 2015;147(1):41-7.
- 33 Wang XS, Zhang Y, He YH, Ma PP, Fan LJ, Wang YC, et al. Aberrant promoter methylation of the CD4 gene in peripheral blood cells of mastitic dairy cows. *Genet Mol Res* 2013;12(4):6228-39.
- 34 Neri F, Rapelli S, Krepelova A, Incarnato D, Parlato C, Basile G, et al. Intragenic DNA methylation prevents spurious transcription initiation. *Nature*. 2017;543(7643):72-7.
- 35 Jeziorska DM, Murray RJS, De Gobbi M, Gaentzsch R, Garrick D, Ayyub H, et al. DNA methylation of intragenic CpG islands depends on their transcriptional activity during differentiation and disease. *Proc Natl Acad Sci U S A* 2017;114(36):E7526-35.
- 36 Köchert K, Ullrich K, Kreher S, Aster JC, Kitagawa M, Jöhrens K, et al. High-level expression of Mastermind-like 2 contributes to aberrant activation of the NOTCH signaling pathway in human lymphomas. *Oncogene* 2011;30(15):1831-40.
- 37 Heynen GJ, Nevedomskaya E, Palit S, Jagalur Basheer N, Liefink C, Schlicker A, et al. Mastermind-Like 3 controls proliferation and differentiation in neuroblastoma. *Mol Cancer Res* 2016;14(5):411-22.
- 38 Muguruma Y, Hozumi K, Warita H, Yahata T, Uno T, Ito M, et al. Maintenance of bone homeostasis by DLL1-Mediated Notch Signaling. *J Cell Physiol* 2017;232(9):2569-80.
- 39 Liu P, Ping Y, Ma M, Zhang D, Liu C, Zaidi S, et al. Anabolic actions of Notch on mature bone. *Proc Natl Acad Sci U S A* 2016;113(15):E2152-61.
- 40 Ramasamy SK, Kusumbe AP, Wang L, Adams RH. Endothelial Notch activity promotes angiogenesis and osteogenesis in bone. *Nature* 2014;507(7492):376-80.
- 41 Salazar VS, Gamer LW, Rosen V. BMP signalling in skeletal development, disease and repair. *Nat Rev Endocrinol* 2016;12(4):203-21.
- 42 Kim JW, Choi H, Jeong BC, Oh SH, Hur SW, Lee BN, et al. Transcriptional factor ATF6 is involved in odontoblastic differentiation. *J Dent Res* 2014;93(5):483-9.
- 43 Li XN, Lv P, Sun Z, Li GS, Xu H. Role of unfolded protein response in affecting osteoblast differentiation induced by fluoride. *Biol Trace Elem Res* 2014;158(1):113-21.